

Supporting Information

for *Adv. Electron. Mater.*, DOI: 10.1002/aelm.201900974

Reversible Tuning of Magnetization in a Ferromagnetic Ruddlesden–Popper-Type Manganite by Electrochemical Fluoride-Ion Intercalation

*Sami Vasala, Anna Jakob, Kerstin Wissel, Aamir Iqbal Waidha, Lambert Alff, and Oliver Clemens**

Supporting Information

Reversible Tuning of Magnetization in a Ferromagnetic Ruddlesden–Popper-Type Manganite by Electrochemical Fluoride-Ion Intercalation

*Sami Vasala, Anna Jakob, Kerstin Wissel, Aamir Iqbal Waidha, Lambert Alff, Oliver Clemens**

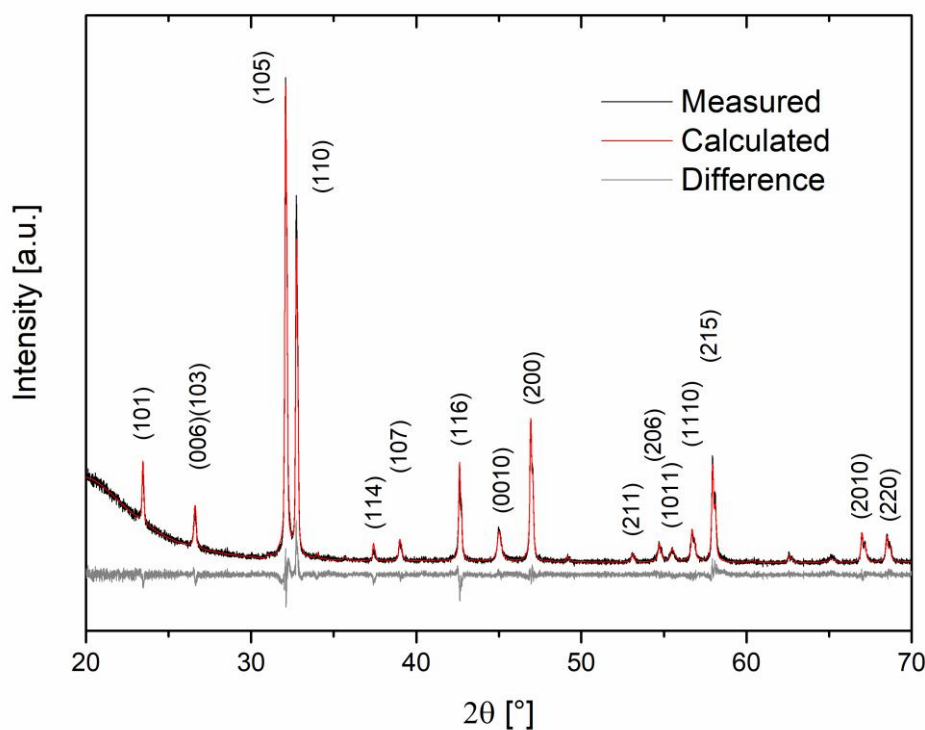


Figure S1. Rietveld refinement for the as-synthesized $\text{La}_{1.3}\text{Sr}_{1.7}\text{Mn}_2\text{O}_7$. The hkl of the most intense reflections are marked.

Table S1. Rietveld refinement results for the as-synthesized $\text{La}_{1.3}\text{Sr}_{1.7}\text{Mn}_2\text{O}_7$. Space group $I4/mmm$. Mn is located at $(0,0,z)$, La,Sr(1) at $(0,0,0.5)$ (perovskite site), La,Sr(2) at $(0,0,z)$ (rock-salt site), O(1) at $(0,0,0)$, O(2) at $(0,0,z)$ and O(3) at $(0,0.5,z)$. Site occupation factors (Occ) for the two La/Sr sites are given. The occupation factors were set-up such that the overall composition corresponded to the nominal one.

a [Å]	3.8745(1)
c [Å]	20.1673(5)
c/a	5.205
V [Å³]	302.75(1)
$z(\text{Mn})$	0.0976(2)
$z(\text{La},\text{Sr}(2))$	0.31599(9)
$z(\text{O}(2))$	0.2052(7)
$z(\text{O}(3))$	0.0923(6)
Occ(La(1))	0.481(9)
Occ(Sr(1))	0.519(9)
Occ(La(2))	0.410(5)
Occ(Sr(2))	0.590(5)
R_p [%]	6.19
R_{wp} [%]	8.24

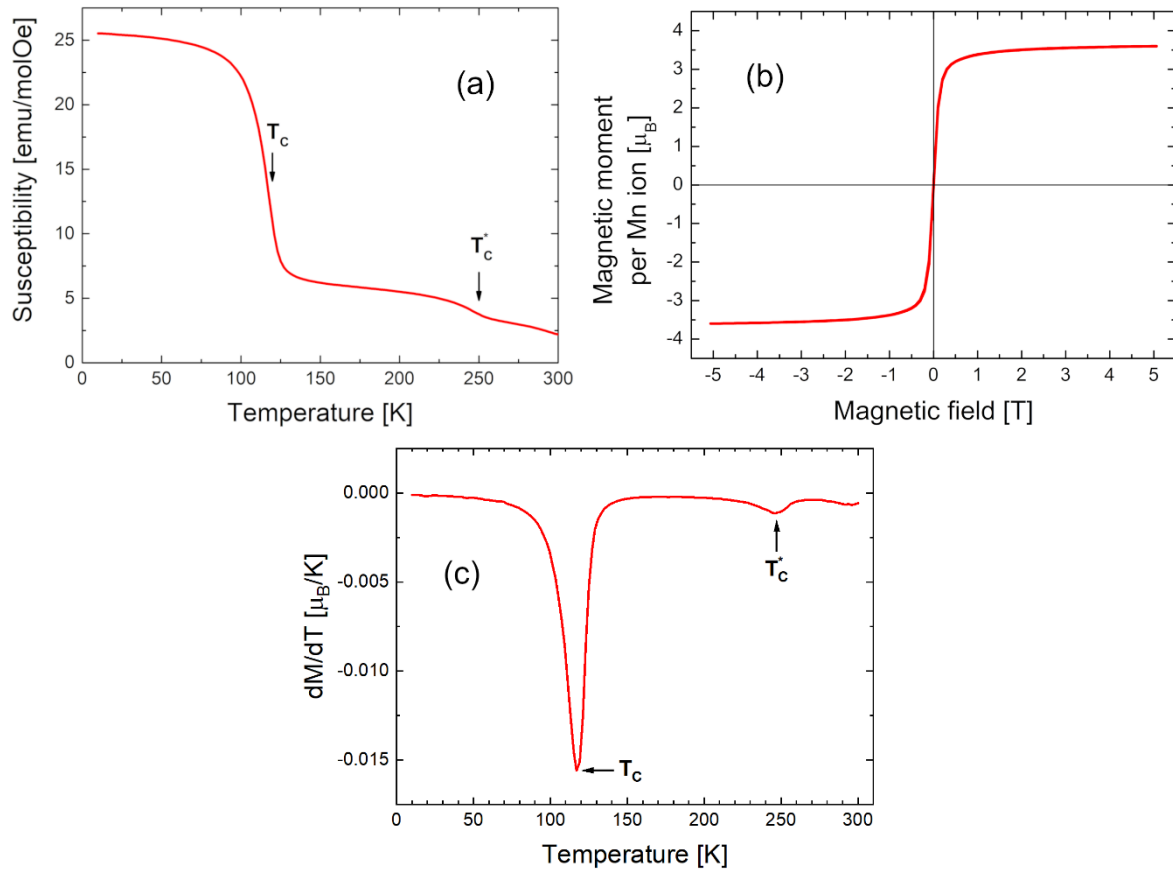


Figure S2: Magnetic properties of the as-synthesized $\text{La}_{1.3}\text{Sr}_{1.7}\text{Mn}_2\text{O}_7$. a) $M(T)$ curve (FC mode, 0.05 T field). b) $M(H)$ hysteresis loop (at 10 K). c) dM/dT curve from which the transition temperatures were determined. The small increase in magnetization at $T_{c^*} \approx 246$ K is a phenomenon observed for numerous systems with similar compositions and has been commonly ascribed to the occurrence of two-dimensional magnetism due to anisotropic exchange interactions.

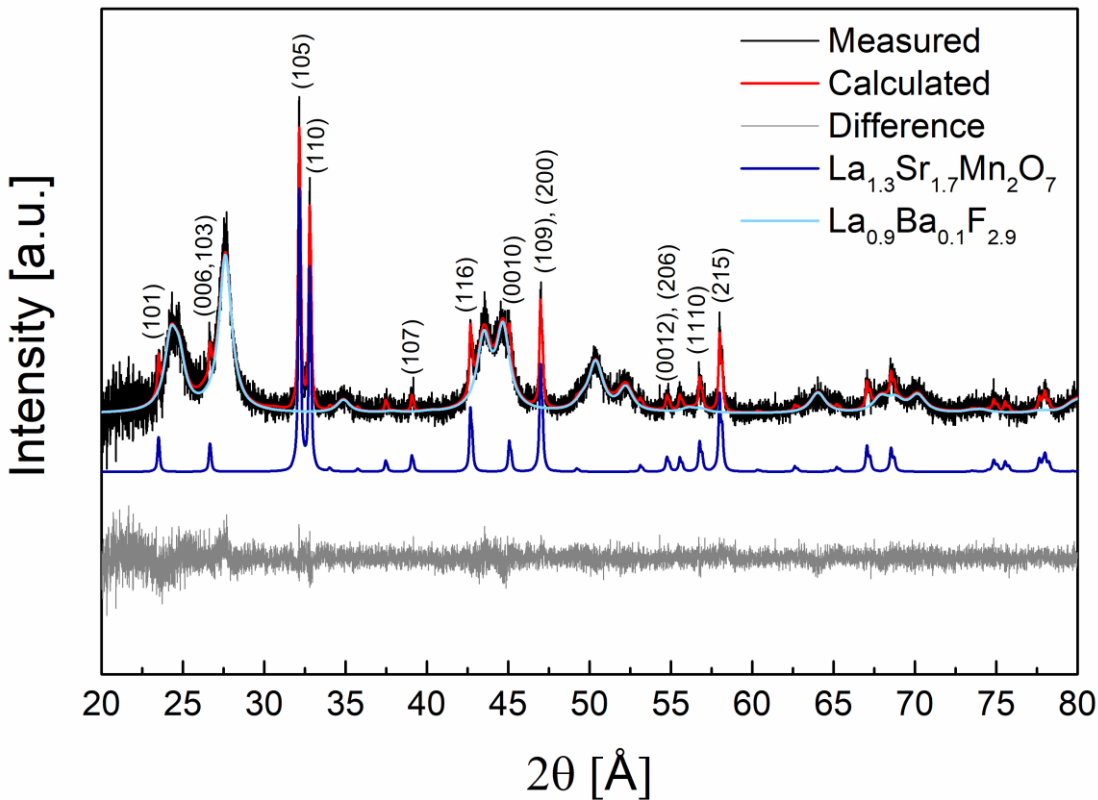


Figure S3: Rietveld refinement of the $\text{La}_{1.3}\text{Sr}_{1.7}\text{Mn}_2\text{O}_7$ cathode composite. The hkl of some reflections belonging to the active material are marked.

Table S2. listing of the lattice parameters obtained for the as-synthesized $\text{La}_{1.3}\text{Sr}_{1.7}\text{Mn}_2\text{O}_7$ sample, the mixed cathode composite and of the heated cathode composite (10 days at 170 °C without charging).

	a [\AA]	c [\AA]	V [\AA^3]
As prepared $\text{La}_{1.3}\text{Sr}_{1.7}\text{Mn}_2\text{O}_7$	3.8745(3)	20.1673(5)	302.75(2)
Cathode composite	3.8755(2)	20.165(1)	302.87(3)
Heated cathode composite	3.8750(2)	20.163(1)	302.77(3)

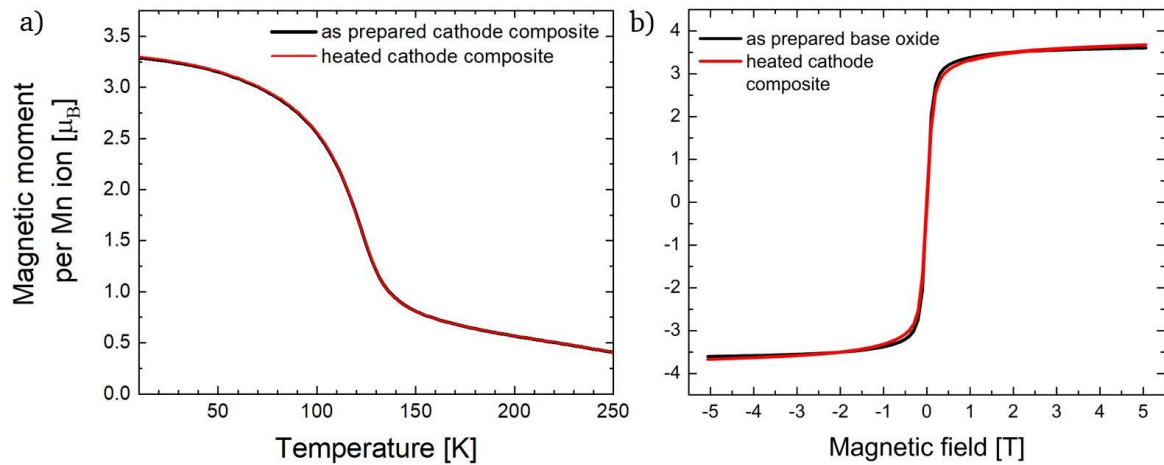


Figure S4: Comparison of the magnetic properties of the as-prepared cathode composite and the heated cathode composite (10 days at 170 °C without charging). a) $M(T)$ curves (FC mode, 1 T field). b) $M(H)$ curves (10 K).

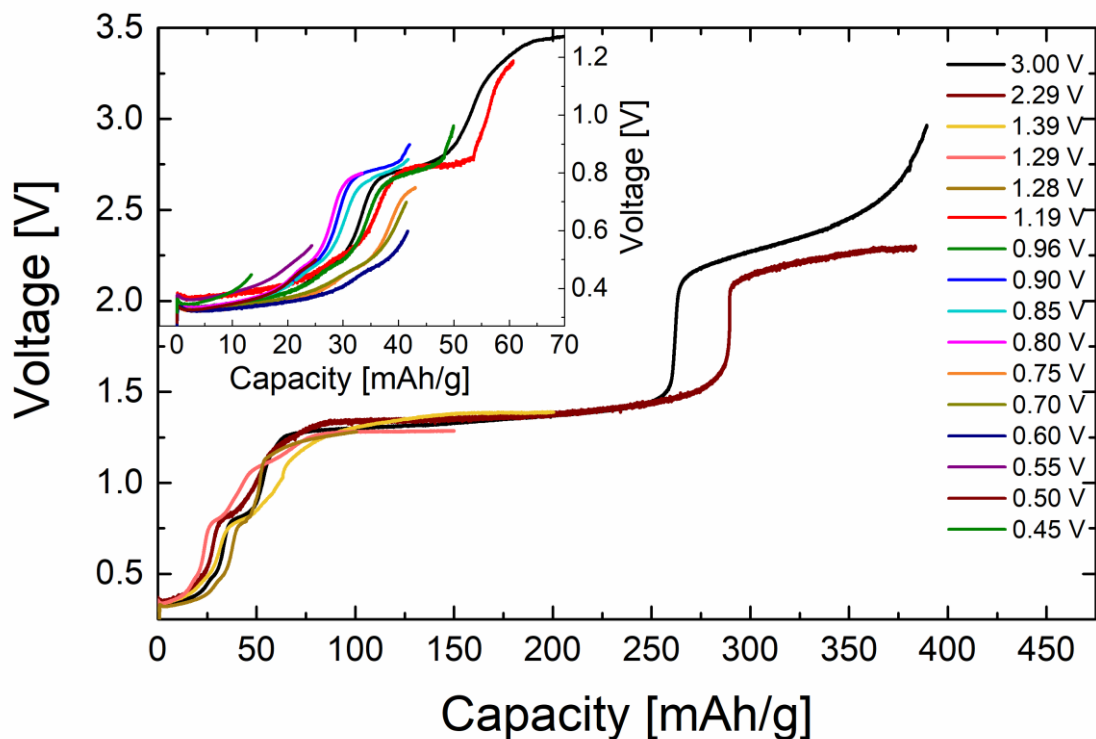


Figure S5: Individual charging curves of the cells charged to selected cut-off voltages. The cells charged to a voltage ≤ 0.9 V are plotted in the inset for better clarity.

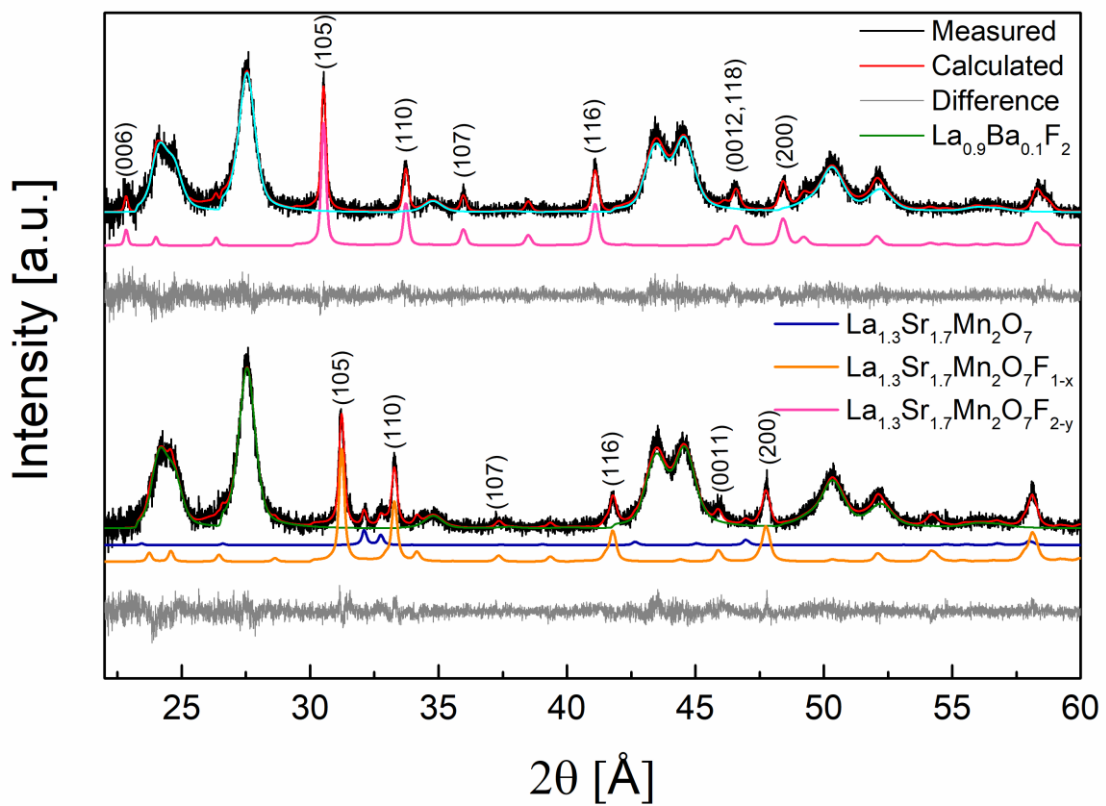


Figure S6. Rietveld refinements for cathode composites charged to (top) 1.19 V or (bottom) 0.55 V.

Table S3. Unit-cell parameters and RWFs for the phases present in cells charged to different cut-off voltages. Refinements for $\text{La}_{1.3}\text{Sr}_{1.7}\text{Mn}_2\text{O}_7\text{F}_{1-x}$ ($P4/nmm$) and $\text{La}_{1.3}\text{Sr}_{1.7}\text{Mn}_2\text{O}_7\text{F}_{2-x}$ ($I4/mmm$) were based on structures presented in references [27, 28].

V_c [V]	$\text{La}_{1.3}\text{Sr}_{1.7}\text{Mn}_2\text{O}_7$ ($I4/mmm$)				$\text{La}_{1.3}\text{Sr}_{1.7}\text{Mn}_2\text{O}_7\text{F}_{1-x}$ ($P4/nmm$)				$\text{La}_{1.3}\text{Sr}_{1.7}\text{Mn}_2\text{O}_7\text{F}_{2-x}$ ($I4/mmm$)			
	a [\AA]	c [\AA]	V [\AA ³]	RWF [%]	a [\AA]	c [\AA]	V [\AA ³]	RWF [%]	a [\AA]	c [\AA]	V [\AA ³]	RWF [%]
0	3.8754(2)	20.165(1)	302.87(3)	100.0				0.0				0.0
0.45	3.8751(4)	20.161(3)	302.74(7)	39.0	3.8201(4)	21.626(4)	315.58(8)	61.0				0.0
0.5	3.871(1)	20.16(1)	302.1(2)	12.2	3.8126(4)	21.776(4)	316.55(9)	87.8				0.0
0.55	3.872(1)	20.14(1)	301.9(3)	10.1	3.8120(4)	21.769(3)	316.33(8)	89.9				0.0
0.6	3.873(2)	20.15(2)	302.3(4)	6.0	3.8040(4)	21.915(3)	317.11(8)	94.0				0.0
0.7				0.0	3.8006(5)	21.944(5)	316.9(1)	100.0				0.0
0.75	3.874(2)	20.09(2)	301.5(4)	3.9	3.7995(5)	21.982(5)	317.3(1)	75.2	3.762(2)	23.26(2)	329.2(4)	20.9
0.8	3.871(1)	20.18(1)	302.4(2)	7.8	3.7997(5)	22.028(5)	318.0(1)	50.3	3.7574(6)	23.406(4)	330.4(1)	41.9
0.85				0.0	3.793(1)	22.17(2)	318.9(3)	21.5	3.7582(4)	23.406(3)	330.58(9)	78.5
0.9				0.0				0.0	3.7622(4)	23.408(3)	331.31(8)	100.0
0.964				0.0				0.0	3.7620(3)	23.425(2)	331.52(6)	100.0
1				0.0				0.0	3.7610(3)	23.449(2)	331.68(6)	100.0
1.19				0.0				0.0	3.7642(4)	23.418(3)	331.81(8)	100.0
1.281				0.0				0.0	3.7669(3)	23.429(3)	332.44(7)	100.0
1.284				0.0				0.0	3.7646(3)	23.620(3)	334.74(7)	100.0
1.286				0.0				0.0	3.7727(3)	23.408(2)	333.16(7)	100.0
1.373				0.0				0.0	3.7703(4)	23.532(4)	334.51(9)	100.0
1.389				0.0				0.0	3.7668(4)	23.477(4)	333.11(8)	100.0
2.292				0.0				0.0	3.7688(3)	23.595(3)	335.14(7)	100.0
2.959				0.0				0.0	3.7650(3)	23.646(3)	335.19(7)	100.0
3				0.0				0.0	3.7697(4)	23.563(3)	334.85(8)	100.0

Table S4: Estimations of the fluoride content for cathode composites charged to cut-off voltages ≤ 0.7 V. The average specific charge capacities for the cells were determined based on the charge curves of the individual cells shown in Figure S5. Based on these values the average fluoride content (related to the whole active material) and the fluoride content of the fluorinated phase (based on the respective RWFs, see Table S3) were calculated.

V_C	Average specific charge capacity [mAh/g]	Average fluoride content	Fluoride content of fluorinated phase [$\text{La}_{1.3}\text{Sr}_{1.7}\text{Mn}_2\text{O}_7\text{F}_y$]
0.45 V	~18	~0.37	~0.61
0.5 V	~26.6	~0.54	~0.62
0.55 V	~28.8	~0.59	~0.66
0.6 V	~30.2	~0.62	~0.66
0.7 V	~32	~0.65	~0.65

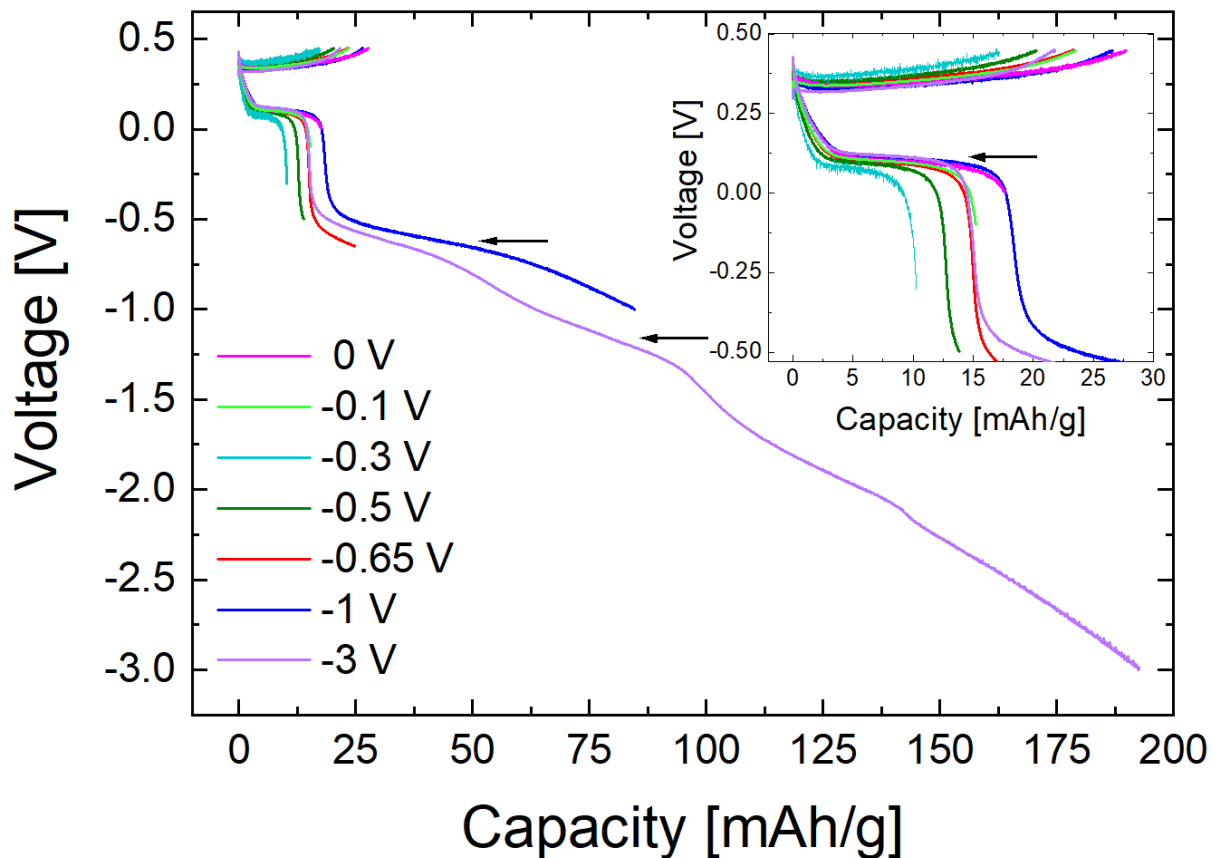


Figure S7. Charge-discharge curves for cells charged to 0.45 V and discharged to selected cut-off voltages.

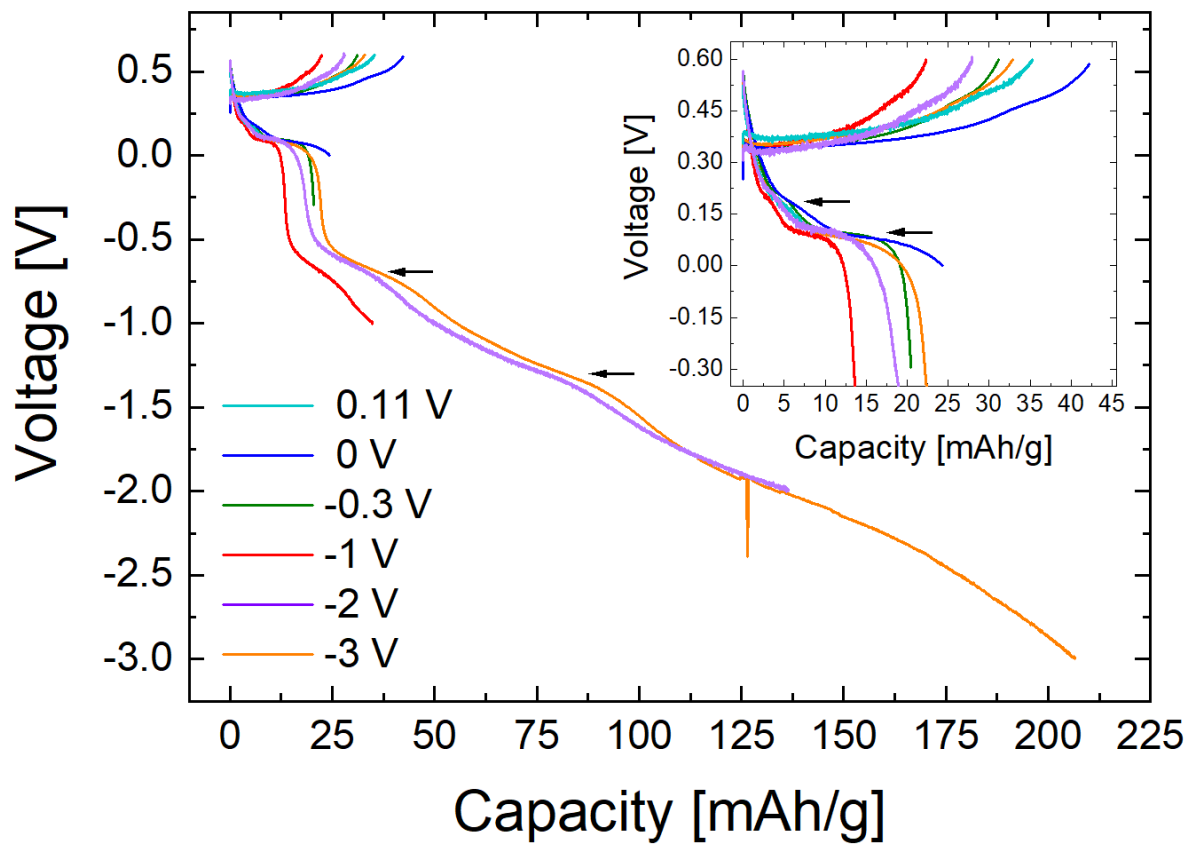


Figure S8. Charge-discharge curves for cells charged to 0.6 V and discharged to selected cut-off voltages.

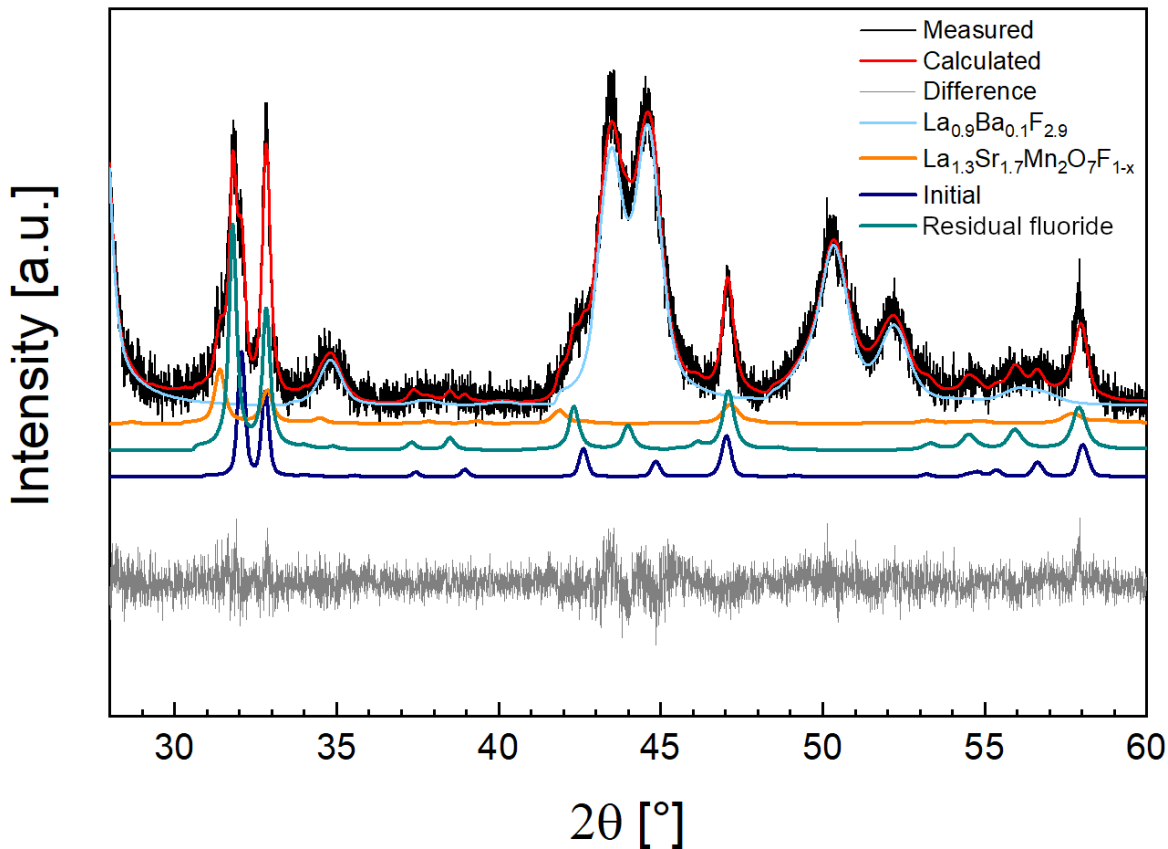


Figure S9. Rietveld refinement for a cathode composite charged to 0.6 V and discharged to -0.3 V.

Table S5. Unit-cell parameters and RWFs for the phases present in cells charged to 0.45 V and discharged to different cut-off voltages. Refinements for residual fluoride phase were based on the La_{1.3}Sr_{1.7}Mn₂O₇ (*I*4/*mmm*) structure.

V_d [V]	La _{1.3} Sr _{1.7} Mn ₂ O ₇ (<i>I</i> 4/ <i>mmm</i>)				Residual fluoride (<i>I</i> 4/ <i>mmm</i>)				La _{1.3} Sr _{1.7} Mn ₂ O ₇ F _{1-x} (<i>P</i> 4/ <i>nmm</i>)			
	a [\AA]	c [\AA]	V [\AA ³]	RWF [%]	a [\AA]	c [\AA]	V [\AA ³]	RWF [%]	a [\AA]	c [\AA]	V [\AA ³]	RWF [%]
0	3.8713(7)	20.203(6)	302.8(1)	43.1	3.867(1)	20.502(9)	306.5(2)	32.8	3.851(2)	21.22(2)	314.7(5)	24.1
-0.1	3.8720(6)	20.193(6)	302.7(1)	53.4	3.865(1)	20.509(8)	306.4(2)	29.1	3.859(2)	21.06(3)	313.7(6)	17.5
-0.3	3.8736(4)	20.175(3)	302.72(7)	58.4	3.867(1)	20.528(7)	306.9(2)	27.9	3.854(3)	21.14(4)	314.0(7)	13.7
-0.5	3.8736(4)	20.171(3)	302.66(8)	53.4	3.866(1)	20.507(7)	306.5(2)	37.4	3.863(3)	21.09(3)	314.7(7)	9.2
-0.56	3.8717(6)	20.205(6)	302.9(1)	37.2	3.8695(8)	20.478(6)	306.6(2)	42.3	3.878(2)	20.89(3)	314.2(6)	20.5
-1	3.873(1)	20.17(1)	302.6(3)	7.6	3.8799(6)	20.451(5)	307.9(1)	92.4				0.0
-3				0.0	3.9051(9)	20.44(1)	311.6(2)	74.3	4.008(6)	21.52(5)	345.7(2)	25.7

Table S6. Unit-cell parameters and RWFs for the phases present in cells charged to 0.6 V and discharged to different cut-off voltages. Refinements for residual fluoride phase were based on the $\text{La}_{1.3}\text{Sr}_{1.7}\text{Mn}_2\text{O}_7$ ($I4/mmm$) structure.

V_d [V]	$\text{La}_{1.3}\text{Sr}_{1.7}\text{Mn}_2\text{O}_7$ ($I4/mmm$)			Residual fluoride ($I4/mmm$)			$\text{La}_{1.3}\text{Sr}_{1.7}\text{Mn}_2\text{O}_7\text{F}_{1-x}$ ($p4/nmm$)						
	a [\AA]	c [\AA]	V [\AA ³]	RWF [%]	a [\AA]	c [\AA]	V [\AA ³]	RWF [%]	a [\AA]	c [\AA]	V [\AA ³]	RWF [%]	
0.11	3.876(2)	20.15(2)	302.8(3)	10.8					0.0	3.8219(3)	21.632(3)	315.98(7)	89.2
0	3.8714(7)	20.189(5)	302.6(1)	23.6	3.862(1)	20.70(1)	308.9(2)	43.5	3.8352(8)	21.484(8)	316.0(2)	32.9	
-0.3	3.869(1)	20.236(8)	302.9(2)	25.2	3.864(1)	20.614(7)	307.8(2)	52.4	3.862(3)	21.20(3)	316.1(7)	22.4	
-1	3.873(1)	20.175(8)	302.6(2)	11.1	3.8776(6)	20.534(5)	308.8(1)	83.8	3.868(4)	21.26(3)	318.1(8)	5.1	
-2	3.868(1)	20.15(1)	301.4(3)	13.3	3.888(2)	20.41(1)	308.5(4)	86.7				0.0	
-3				0.0	3.914(2)	20.32(1)	311.3(3)	100.0				0.0	

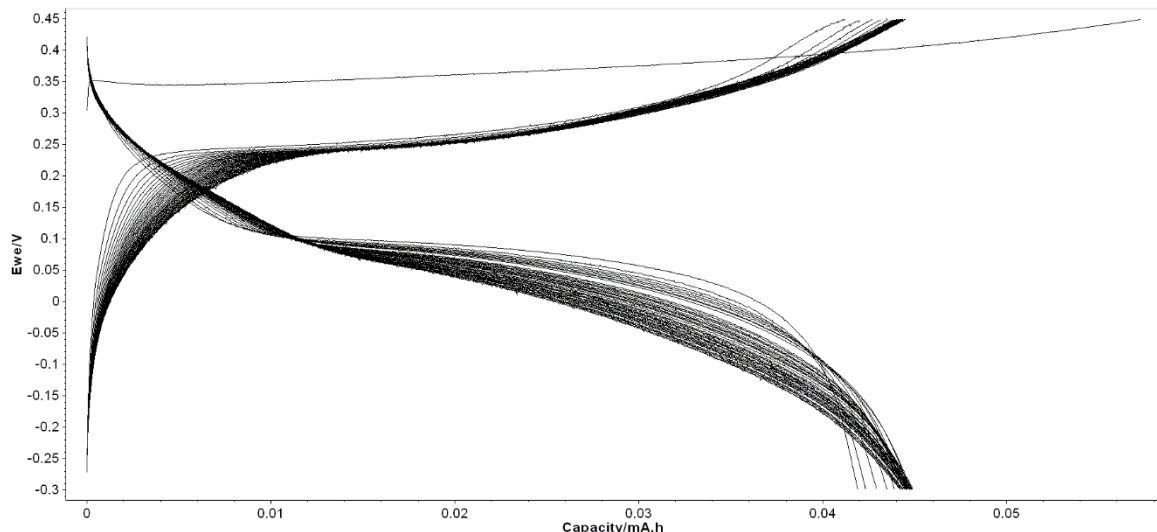


Figure S10. Capacity-voltage curves for the cell operated for 45 cycles between 0.45 and -0.3 V.

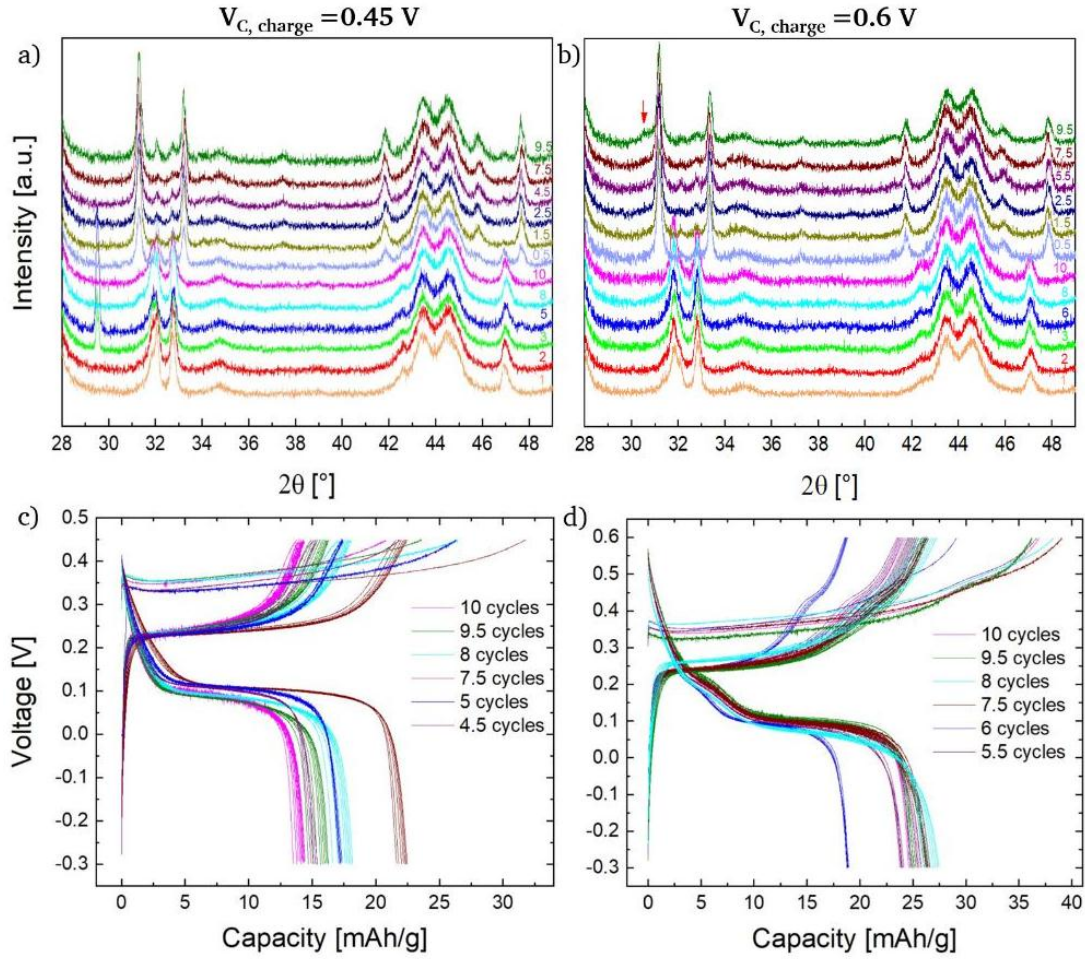


Figure S11. (a),(b) Diffraction patterns of cells operated for different number of cycles with (a) $V_{C,\text{charge}} = 0.45 \text{ V}$ and (b) 0.6 V and $V_{C,\text{discharge}} = -0.3 \text{ V}$. The red arrow in (b) indicates the (105) reflection of the arising $\text{La}_{1.3}\text{Sr}_{1.7}\text{Mn}_2\text{O}_7\text{F}_{2-x}$ ($I4/\text{mmm}$) phase. The reflection around 29.5° belongs to the silicon plate of the sample holder. The corresponding capacity-voltage curves for the cells operated ≥ 4.5 cycles are depicted in (c) and (d).

Table S7. Unit-cell parameters and RWFs for the phases present in cells cycled between 0.45 and -0.3 V.

Cycle number	La _{1.3} Sr _{1.7} Mn ₂ O ₇ (I4/mmm)				Residual fluoride (I4/mmm)				La _{1.3} Sr _{1.7} Mn ₂ O ₇ F _{1-x} (P4/nmm)			
	<i>a</i> [Å]	<i>c</i> [Å]	<i>V</i> [Å ³]	RWF [%]	<i>a</i> [Å]	<i>c</i> [Å]	<i>V</i> [Å ³]	RWF [%]	<i>a</i> [Å]	<i>c</i> [Å]	<i>V</i> [Å ³]	RWF [%]
0.5	3.8751(4)	20.161(3)	302.74(7)	39.0				0.0	3.8201(4)	21.626(4)	315.58(8)	61.0
1.5	3.878(2)	20.17(1)	303.4(3)	11.9				0.0	3.8189(3)	21.677(3)	316.15(7)	88.1
2.5	3.879(1)	20.16(1)	303.3(3)	11.2				0.0	3.8216(4)	21.611(3)	315.62(8)	88.8
4.5	3.877(2)	20.14(2)	302.8(4)	15.9				0.0	3.8221(8)	21.592(6)	315.4(2)	84.1
4.5	3.876(1)	20.16(1)	302.9(3)	10.9				0.0	3.8198(3)	21.665(3)	316.12(7)	89.1
7.5	3.877(2)	20.13(2)	302.6(5)	6.5				0.0	3.8177(3)	21.703(3)	316.32(7)	93.5
9.5	3.8774(9)	20.172(9)	303.3(2)	11.1				0.0	3.8209(3)	21.637(3)	315.88(7)	88.9
1	3.8737(3)	20.175(3)	302.74(7)	53.2	3.867(1)	20.518(7)	306.8(2)	36.3	3.860(3)	21.08(3)	314.0(7)	10.5
2	3.8725(4)	20.180(4)	302.62(9)	54.5	3.867(1)	20.515(8)	306.7(2)	34.6	3.869(4)	20.99(4)	314.1(8)	11.0
3	3.8720(8)	20.185(7)	302.6(2)	54.1	3.867(1)	20.483(8)	306.2(2)	28.4	3.865(3)	20.88(3)	312.0(6)	17.5
5	3.870(1)	20.23(1)	303.2(3)	57.6	3.868(2)	20.52(2)	307.0(4)	31.4	3.860(4)	20.97(4)	312.5(9)	11.0
8	3.8707(7)	20.211(6)	302.8(1)	38.4	3.867(1)	20.528(6)	307.0(2)	38.8	3.863(2)	21.07(2)	314.5(5)	22.8
10	3.8728(5)	20.188(4)	302.79(9)	45.0	3.8660(9)	20.529(7)	306.8(2)	29.3	3.857(2)	21.16(3)	314.9(6)	25.6

Table S8. Unit-cell parameters and RWFs for the phases present in cells cycled between 0.6 and -0.3 V. The cell operated for 9.5 cycles also contained a small fraction (RWF = 11.3 %) of La_{1.3}Sr_{1.7}Mn₂O₇F_{1-x} (*a* = 3.796(2) Å, *c* = 23.14(2) Å).

Cycle number	La _{1.3} Sr _{1.7} Mn ₂ O ₇ (I4/mmm)				Residual fluoride (I4/mmm)				La _{1.3} Sr _{1.7} Mn ₂ O ₇ F _{1-x} (P4/nmm)			
	<i>a</i> [Å]	<i>c</i> [Å]	<i>V</i> [Å ³]	RWF [%]	<i>a</i> [Å]	<i>c</i> [Å]	<i>V</i> [Å ³]	RWF [%]	<i>a</i> [Å]	<i>c</i> [Å]	<i>V</i> [Å ³]	RWF [%]
0.5	3.873(2)	20.15(2)	302.3(4)	6.0				0.0	3.8040(4)	21.915(3)	317.11(8)	94.0
1.5	3.873(1)	20.14(1)	302.1(3)	5.8				0.0	3.8064(3)	21.887(3)	317.12(7)	94.2
2.5	3.873(2)	20.17(2)	302.6(5)	3.9				0.0	3.8057(3)	21.904(3)	317.24(6)	96.1
5.5	3.870(1)	20.13(1)	301.5(3)	6.3				0.0	3.8039(4)	21.886(3)	316.68(8)	93.7
7.5	3.877(2)	20.11(2)	302.3(5)	2.1				0.0	3.8064(3)	21.905(3)	317.37(7)	97.9
9.5	3.874(2)	20.10(2)	301.7(5)	5.1				0.0	3.8069(4)	21.888(3)	317.23(8)	83.6
1	3.868(1)	20.260(9)	303.2(2)	35.0	3.8641(9)	20.625(6)	307.9(2)	41.0	3.863(3)	21.14(3)	315.6(6)	24.0
2	3.867(1)	20.28(1)	303.3(3)	31.9	3.8637(9)	20.613(6)	307.7(2)	48.4	3.862(3)	21.11(2)	314.8(5)	19.6
3	3.868(1)	20.30(1)	303.7(3)	33.6	3.866(1)	20.587(7)	307.7(2)	49.1	3.865(3)	21.05(3)	314.5(6)	17.3
6	3.868(1)	20.32(1)	303.9(3)	40.4	3.863(1)	20.634(7)	308.0(2)	43.5	3.861(3)	21.09(3)	314.4(7)	16.1
8	3.869(1)	20.36(1)	304.7(3)	39.4	3.8678(9)	20.615(7)	308.4(2)	38.1	3.869(3)	20.92(3)	313.2(6)	22.5
10	3.867(2)	20.37(2)	304.5(3)	29.8	3.866(1)	20.634(7)	308.4(2)	49.8	3.869(3)	21.11(3)	316.1(6)	20.4

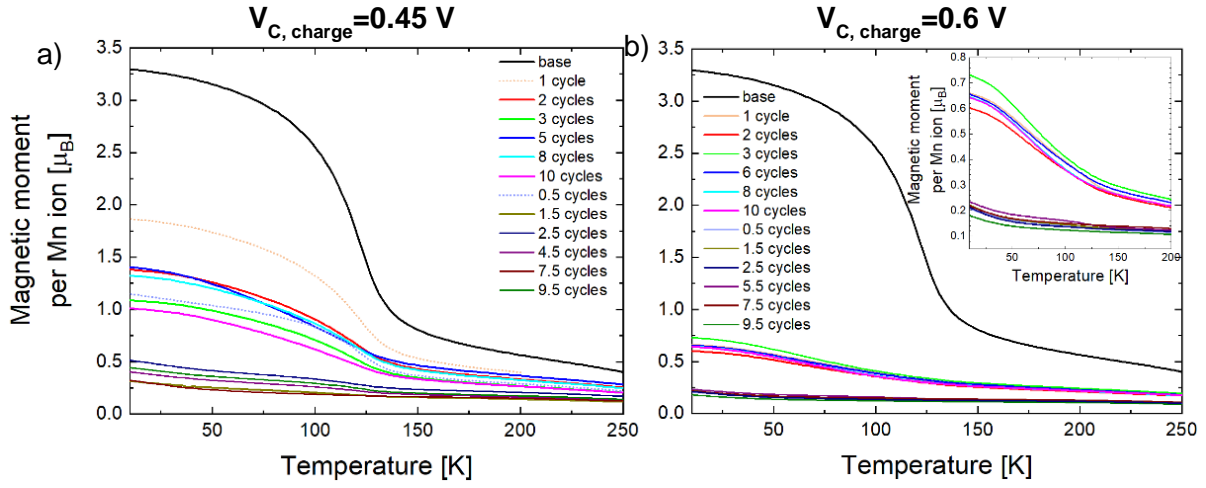


Figure S12. $M(T)$ curves (FC mode, 1 T field) for cathode composites operated for different number of cycles with (a) $V_{C, \text{charge}} = 0.45 \text{ V}$ and (b) 0.6 V. The magnetic data of the heated cell ($170 \text{ }^{\circ}\text{C}$, 10 days) is given as a reference ('base'). For $V_{C, \text{charge}} = 0.45 \text{ V}$ the first cycle is shown with dotted lines to clarify that the system stabilizes from the second cycle onwards.

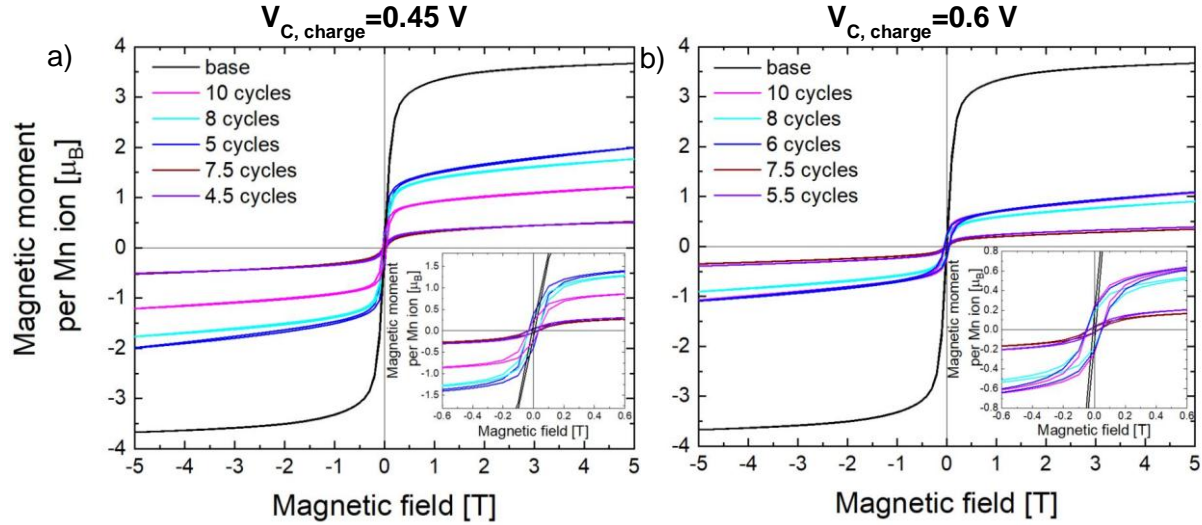


Figure S13: $M(H)$ curves (10 K) for cathode composites operated for different number of cycles with (a) $V_{C, \text{charge}} = 0.45 \text{ V}$ and (b) 0.6 V. The insets show that the discharged cells exhibit a small hysteretic behavior as compared to the heated-only material ('base').